

Quantum resonances and decay of a chaotic fractal repeller observed using microwaves

Wentao Lu, M.Rose, K.Pance and S.Sridhar^a
Physics Department, 360 Huntington Avenue, Boston, MA 02115.
 (August 9, 2018)

The quantum resonances of classically chaotic n-disk geometries were studied experimentally utilizing thin 2-D microwave geometries. The experiments yield the frequencies and widths of low-lying resonances, which are compared with semiclassical calculations. The longtime or small energy behavior of the wave-vector auto-correlation gives information about the quantum decay rate, which is in good agreement with that obtained from classical scattering theory. The intermediate energy behavior shows non-universal oscillations determined by periodic orbits.

The n-disk scattering problem is one whose quantum-classical correspondence has received extensive theoretical attention [1,2], because it is a paradigm of an open quantum chaos system, much as the pendulum is for integrable systems. Furthermore it is relevant to physical situations in diverse fields, such as the crossroads geometry for electron devices [3], unimolecular chemical reactions [2] and electromagnetic and acoustic scattering [4].

The classical scattering function of n-disks on a plane is non-differentiable and forms a Cantor set. A central property is the exponential decay of an initial distribution of classical particles, hence the name (fractal) repeller. For closed quantum chaotic billiards, experimental and theoretical work is available on eigenvalues (which are purely real) and eigenfunctions, and the many features of universality and non-universal behavior are known [5]. In contrast, for open quantum systems, the eigenvalues are intrinsically complex and their universal behavior is a question of great interest [6]. Despite extensive theoretical treatment there have been almost no real experiments on the n-disk geometry which exemplify this unique problem in quantum chaos.

In this paper we present a microwave realization of the chaotic n-disk problem. Experiments were carried out for $n = 1, 2, 3, 4, 6$, as well as for large $n = 20$, the latter corresponding to the random Lorentz scatterer. In this paper we focus on the case $n = 4$. The experiments yield the frequencies and the widths of the low lying quantum resonances of the four-disk repeller. We have also carried out semiclassical calculations of the resonances, which are shown to reproduce the resonances reasonably well. Our experiments enable us to explore the role of symmetry in a unique way by studying different irreducible representations. The experimental data are used to display the signatures of the classical chaos in the transmission spectra, through measures such as the spectral (wave-vector k) auto-correlation function. The small k (long time) behavior of this quantity provides a measure of the quantum escape rate, and is shown to be in good agreement with the corresponding classical escape rate. For large k (short times), the contribution of periodic orbits is observed as

non-universal oscillations of the auto-correlation.

The experiments are carried out in thin microwave structures consisting of two highly conducting *Cu* plates spaced $d \sim 6\text{ mm}$ and about $55 \times 55\text{ cm}$ in area. Discs and bars also made of *Cu* and of thickness d are placed between the plates and in contact with them. In order to simulate an infinite system microwave absorber material was sandwiched between the plates at the edges. Microwaves were coupled in and out using loops terminating coaxial lines which were inserted in the vicinity of the scatterers. All measurements were carried out using an HP8510B vector network analyzer which measured the complex transmission (S_{21}) and reflection (S_{11}) S-parameters of the coax + scatterer system. It is crucial to ensure that there is no spurious background scattering due to the finite size of the system. This was verified carefully as well as that the effects of the coupling probes were minimal and did not affect the results.

In this essentially 2-D geometry, Maxwell's equation for the experimental system is identical with the Schrödinger time-independent wave equation $(\nabla^2 + k^2)\Psi = 0$ with $\Psi = E_z$ the z -component of the microwave electric field. This correspondence is exact for all frequencies $f_c < c/2d = 25\text{GHz}$. (Note that $k = 2\pi f/c$, where c is the speed of light). It is this mapping which enables us to study the quantum properties of the n-disk system. For all metallic objects in the 2-D space between the plates, Dirichlet boundary conditions apply inside the metal. Thus for the 4-disk geometry, $\Psi = 0$ inside the 4 disks.

The transmission function $S_{21}(f)$ which we measure is the response of the system to a delta-function excitation at point \vec{r}_1 probed at a different point \vec{r}_2 , and is determined by the wavefunction Ψ at the probe locations \vec{r}_1 and \vec{r}_2 . In our experiments the coax lines act as tunneling point contacts, and hence it can be shown [7] that $S_{21}(f) = A(f)G(\vec{r}_1, \vec{r}_2, f)$ is just the two-point Green's function $G(\vec{r}_1, \vec{r}_2, f)$, scaled by a slowly varying function $A(f)$ of frequency f which represents the impedance characteristics of the coax lines and probes. Because we ensure that the coupling to the leads is very

weak, any shifts due to the leads are negligible ($< 10^{-4}$ of the resonance frequencies and widths) [8].

Note that the measurements of $|S_{21}(f)|^2$ are equivalent to a two-probe measurement of the conductance [3], since the conductance $g \propto \sum |t_{nm}|^2$, the sum of the transmission probabilities t_{nm} for all input/output channels (n, m). In the present experiment, the input/output leads are δ -function point contacts, and hence $t_{11} = S_{21}$ and $g \propto |S_{21}(f)|^2$. Thus our experiments enable us to make comparison with theories [3,9–11] originally developed for electronic micro-structures [12,13].

The transmission function $|S_{21}|^2$ for a square 4-disk system with disk radius $a = 2\text{cm}$ and separation $R = 8\text{cm}$ is shown in Fig.1. The data shown is the sum of traces taken for 3 locations of the probes, in order to avoid accidental zeros of the wavefunction at the probe locations. Several resonances are clearly seen. The resonance frequencies f and widths Δf directly yield the complex wave-vector quantum eigenvalues of the 4-disk repeller. In our previous experiments on closed cavities such as Sinai billiard geometries [14], the widths of the eigen-resonances were due to dissipation in the metal walls. Here however the resonance widths are due to decay of the wavefunction into infinite space. These experiments thus enable us to explore quantum decay in open systems. It must be emphasized that the dissipation in the walls is entirely negligible in the present experiments.

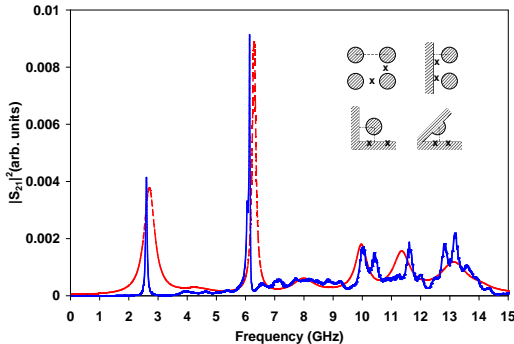


FIG. 1. Transmission function $|S_{21}|^2$ for a 4-disk system with $R = 8\text{cm}$ and $a = 2\text{cm}$. The dashed line is the semi-classical calculation. (Inset) the experimental configuration and the various reduced representations of the 4-disk geometries studied in this work. The separation distance R is shown as a dashed line. The x's mark typical locations of the coupling probes.

The experimental approach was validated by measurements (not shown) on an (integrable) 2-disk system, for which we have measured both in the full space with two actual disks (A_1 and A_2 representations) and in the half-space using a reflecting mirror (A_2 representation). Here the spectrum consists of a 1-parameter family of resonances due to a single periodic orbit. The experimental data are in very good agreement with semiclassical cal-

culations (for preliminary measurements, see [15]).

For the chaotic 4-disk case, we have also carried out semiclassical calculations using methods in the literature [1,2,16–20]. In the semiclassical theory, the resonances of the system are given by the poles of the Ruelle ζ function with j running from 0 to ∞ [17]

$$\zeta_{(1/2)+j}(-ik) = \prod_p \left[1 - (-1)^{L_p} e^{ikl_p} / \Lambda_p^{(1/2)+j} \right]^{-1} \quad (1)$$

where k is the wave vector, l_p is the length of the periodic orbit p , L_p the number of collisions of the periodic orbit with the disks, and Λ_p is the eigenvalue of the stability matrix.

For the 4-disk system with C_{4v} symmetry, the semi-classical calculations using the cycle expansions [1] were carried out up to period 3 including 14 periodic orbits. Because of the C_{4v} symmetry, there are five representations of the Ruelle ζ function [20], A_1 , A_2 , B_1 , B_2 , E , where the last one is two-dimensional. The poles of the first Ruelle ζ function with $j = 0$ are calculated, since they contribute to the resonances with the longest lifetimes. The energy of the particle is $E = k^2$ (here we can take $m = 1/2$, $\hbar = 1$), and is also complex.

In Fig.1, we show the results of the semi-classical calculations, as a superposition of Lorentzians $S_{cal}^2(k) = \sum_i c_i \gamma_i / ((k - s_i)^2 + \gamma_i^2)$, where s_i and γ_i are the calculated real and imaginary parts of resonances, respectively. The coupling constants c_i were chosen to fit the data - as explained above they are specific to the probe locations. Good agreement is found for the resonance frequencies of the sharp resonances. The sharp resonances with small imaginary parts and hence high Q are easily recognized while the resonances with large imaginary parts are not easy to distinguish, although all resonances contribute to the transmission function in Fig.1.

The approximate semiclassical theory used provides a fair prediction of the resonance frequencies even for the low-lying resonances. The accuracy is within 5%. But the agreement for the widths is not as good as that for the resonance frequencies. The lower the frequency, the greater the discrepancy between the calculated and experimental widths. The discrepancy may improve if more orbits of higher period are included. Another source of the discrepancy is intrinsic in the semi-classical theory because of the large correction of the stationary phase approximation [21]. Comparison with exact quantum calculations [17,4] would be desirable.

One of the noteworthy features of the experiments is the ability to vary geometry. We exploited this by exploring the role of the symmetry in the 4-disk geometry. We performed the experiment in four different setups (see inset to Fig.1). These correspond to four different ways of probing the phase space: the full space in which all five representations are included, half (A_2, B_2, E), one fourth (B_1, B_2), and one eighth of the space (B_2). Ap-

proximately 17 configurations were studied and analyzed in details. The systematic trends are consistent with expectations. Here we discuss some of the principal features of the results, further extensive details will be published in a longer publication [7].

We now turn to another analysis of the data in terms of the spectral auto-correlation function, which was calculated as $C(\kappa) = \langle |S_{21}(k - (\kappa/2))|^2 |S_{21}(k + (\kappa/2))|^2 \rangle_k$. The average is carried out over a band of wave vector centered at certain value k_0 and of width Δk . The window function [22] chosen was $f(x) = (1 - |x|/\sqrt{6})/\sqrt{6}$ for $|x| < \sqrt{6}$ and $f(x) = 0$ for $|x| \geq \sqrt{6}$ with $x = (k - k_0)/\Delta k$. The trace S_{21} used is the average of several traces collected at different probe locations with the same geometrical configuration of the disks to avoid missing resonances due to the accidental coincidence of either probe with a node of the wavefunction. The autocorrelation is the average of that for several k_0 . A plot of the autocorrelation for the 1/8th configuration of the 4-disk geometry is shown in Fig.2.

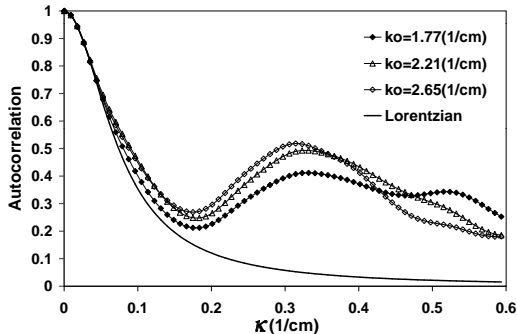


FIG. 2. Wave-vector autocorrelation $C(\kappa)$ of the 4-disk system with $R = 20\text{cm}$ and $a = 5\text{cm}$. Data are shown for 1/8th configuration of the 4-disk geometry corresponding to the B_2 representation. The correlation is calculated with interval $\Delta k = 2\text{cm}^{-1}$. The different sets represent different values of the central wave-vector k_0 . The bold line is a Lorentzian with $\gamma_{qm} = 0.075\text{cm}^{-1}$.

Since $|S_{21}(k)|^2 = \sum_i c_i \gamma_i / ((k - s_i)^2 + \gamma_i^2)$, we have [23] $C(\kappa) = \pi \sum_{i,j} c_i c_j (\gamma_i + \gamma_j) / ((\kappa - (s_i - s_j))^2 + (\gamma_i + \gamma_j)^2)$. In the case that there are no overlapping resonances, $|s_i - s_j| \gg (\gamma_i + \gamma_j)$, the small κ behavior of the auto-correlation is $C(\kappa) \approx \pi \sum_i 2c_i^2 \gamma_i / (\kappa^2 + 4\gamma_i^2)$.

According to semiclassical theory, the above sum can be replaced by a single Lorentzian [24,3,25,22]

$$C(\kappa) = C(0) \frac{1}{1 + (\kappa/\gamma)^2}. \quad (2)$$

In semi-classical theory, $\gamma = \gamma_0$, the classical escape rate with the velocity scaled to 1. Thus one can interpret the width of the autocorrelation as an average lifetime of resonances [26,27]. The above equation was used to fit the spectral autocorrelation for small κ and thus obtain

the value of the experimental escape rate γ_{qm} , as shown in Fig.2.

In the classical scattering theory, the classical escape rate γ_0 is the simple pole of the classical Ruelle ζ function [16]. We use the results of ref. [16] in Fig.3 for comparison with the experimental data. Asymptotically, when R is large, $\gamma_0 \approx \ln(2\sqrt{2}R/a)/(\sqrt{2}R)$. Another relevant quantity is the abscissa of absolute convergence s_c for Eq. (1) which can also be estimated from the Ruelle ζ function with the classical cycle weights t_p replaced by the corresponding semiclassical ones. s_c serves as a lower bound of the escape rate [28], and is also shown in Fig.3. (Note that this is negative for $R/a < 4.5$).

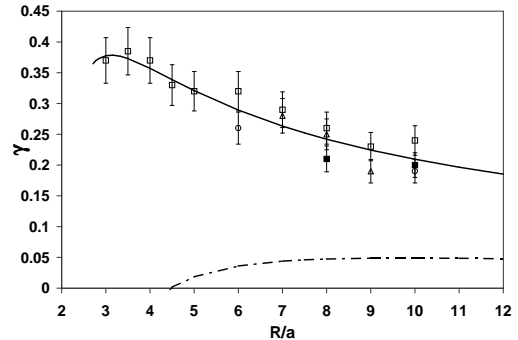


FIG. 3. Experimental escape rate γ_{qm} scaled to radius $a = 1$ versus R/a . Data are shown for different reduced configurations of the 4-disk geometry : 1/8th space(open squares), 1/2 space (open circles), 1/4 space (filled squares), full space (triangles). The classical escape rate (solid line) is calculated from the first three periodic orbits in the fundamental domain. The abscissa of convergence s_c of Eq.(1) is shown as a dot-dashed line, and represents a lower bound on the quantum escape rate.

Good agreement of the escape rate is obtained between that of the classical theory γ_0 and that from the experimental data γ_{qm} . This is shown in Fig.3, where we compare the experimental escape rates γ_{qm} with the classical escape rate γ_0 for several values of R/a . Note that in Fig.3, data are included for 17 configurations of the different reduced (1/8, 1/4, 1/2 and full space) representations of the 4-disk geometry shown in Fig.1. The radius of the disks used was $a = 5\text{cm}$ for the 1/8 space, and $a = 2\text{cm}$ for the others. The data for γ_{qm} are scaled to radius $a = 1$. In Fig.3 we have shown experimentally that the small κ behavior of the spectral auto-correlation has a universal behavior in that it is independent of the details of the geometry. The good agreement in Fig.3 between the measured escape rate γ_{qm} and the classical escape rate γ_0 shows that some quantum properties are well predicted by semiclassical theory.

For intermediate κ , the semiclassical theory Eq.(2) fails because of the presence of the periodic orbits, which lead to non-universal behavior. In the case of just one periodic

orbit, $C(\kappa) \propto \sum_{n=0}^{\infty} 2\gamma/[(\kappa - n\Delta s)^2 + 4\gamma^2]$. For example for the 2-disk problem if just the A_2 representation is present [15], $\Delta s = 2\pi/(R - 2a)$, $2\gamma = \ln \Lambda/(R - 2a)$ is the width of the resonances with the eigenvalue of the instability matrix $\Lambda = [R - a + \sqrt{R(R - 2a)}]/a$. 2γ is also the classical escape rate γ_0 of the system. Thus the autocorrelation oscillates exactly with period Δs . Excellent agreement is found between experiment and theory for this 2-disk case.

In the full space of the 4-disk system, the average length of the periodic orbits per period can be estimated as the average length of the eight periodic orbits, 12, 23, 34, 41, 1234, 1432, 13, 24, where 1, 2, 3, 4 are the labels of the four disks [20]. The mean separation between the resonances is approximately given by $\overline{\Delta s} = 2\pi/[(2 + 1/\sqrt{2})R - (3 + \sqrt{2})a]$. For the 4-disk system with one-eighth of the phase space, the mean separation is $\overline{\Delta s} = 6\pi/[(3 + \sqrt{2})R - 2(2 + \sqrt{2})a]$. The autocorrelation will oscillate with approximate period $\overline{\Delta s}$, which indicates the deviation from the semiclassical theory because of the presence of the periodic orbits in the system. Thus the short time behavior is system specific. The value of $\overline{\Delta s} = 0.35 \text{ cm}^{-1}$ is in good agreement with the scale of oscillations in Fig.2. Future work will focus on the interplay between the universal chaotic features and the non-universal PO contributions.

It is interesting to examine the variation of the results with increasing n . For $n = \infty$ one obtains the Lorentz scatterer. For $n = 20$, we find that $\gamma_{fit} \sim 0.05$, indicating that as n increases the system approaches a closed system and the escape rate becomes very small.

To our knowledge this work represents the first determination of the wave-vector autocorrelation for an experimental system. Our results thus nicely complement measurements in semiconductor microstructures [12,3,13], where however the wave-vector correlation is difficult to extract but instead the magnetic field correlations of conductivity $g(\Delta B)$ are analyzed. As noted previously, the present experiment exactly corresponds to an ideal non-interacting electron in a quantum dot, with tunneling contacts. Thus Fig.1 can be viewed as equivalent to conductivity fluctuations in a quantum dot.

The present work has provided the first experimental realization of the n-disk open billiards problem. *The experiments clearly demonstrate the quantum-classical correspondence, in that the quantum properties can be obtained from classical quantities and vice-versa.* One of the powerful features of the present experiments is the (almost unlimited) ability to vary geometry, as we have already demonstrated by studying numerous configurations. Hence there is enormous potential for addressing a variety of issues in the quantum-classical correspondence problem. In addition open billiards are also a paradigm for dissipative quantum systems, a problem of wide importance. Besides their relevance to atomic and chemical physics, the present results also have applicability to sit-

uations where wave mechanics plays a role, such as in electromagnetism and acoustics.

This work was supported by NSF-PHY-9722681. We thank A. Kudrolli, V. Kidambi, J. V. Jose, N. Whelan and L. Viola for useful discussions.

^a electronic address : srinivas@neu.edu.

- [1] P. Cvitanović, Phys. Rev. Lett. **61**, 2729(1988).
- [2] P. Gaspard and S. A. Rice, J. Chem. Phys. **90**, 2225(1989); **90**, 2242(1989); **90**, 2255(1989); **91**, E3279(1989).
- [3] R. A. Jalabert, H. U. Baranger, and A. D. Stone, Phys. Rev. Lett. **65**, 2442(1990).
- [4] Y. Decanini, A. Folacci, E. Fournier and P. Gabrielli, J. Phys. A: **31**, 7865(1998); **31**, 7891(1998).
- [5] O. Bohigas, in *Chaos and Quantum Physics*, edited by M.-J. Giannoni, A. Voros, and J. Zinn-Justin (Elsevier Science, New York, 1990), and references therein.
- [6] W. Hohn, B. Milek, H. Schanz and P. Seba, Phys. Rev. Lett. **67**, 1949 (1991).
- [7] W. T. Lu, M. Rose, S. Sridhar (in preparation).
- [8] J. Stein, H.-J. Stöckmann and U. Stoffregen, Phys. Rev. Lett. **75**, 53(1995).
- [9] Y. Alhassid and Y. Fyodorov, chao-dyn 9808003.
- [10] W. A. Lin and R. V. Jensen, Phys. Rev. B **53**, 3638 (1996).
- [11] C. D. Schwieters, J. A. Alford, and J. B. Delos, Phys. Rev. B **54**, 10652 (1996), M. W. Beims, V. Kondratovich, and J. B. Delos, Phys. Rev. Lett. **81**, 4537(1998).
- [12] C. M. Marcus, A. J. Rimberg, R. M. Westervelt, P. F. Hopkins, and A. C. Gossard, Phys. Rev. Lett. **69**, 506 (1992).
- [13] A. M. Chang, H. U. Baranger, L. N. Pfeiffer, and K. W. West, Phys. Rev. Lett. **73**, 2111 (1994).
- [14] S. Sridhar, Phys. Rev. Lett. **67**, 785(1991).
- [15] A. Kudrolli and S. Sridhar, in J.-M. Yuan, *et. al.*, ed, *Proc. 4th Drexel Conf.* (Singapore: World Scientific).(1998).
- [16] P. Gaspard and D. Alonso, Phys. Rev. A **45**, 8383(1992).
- [17] P. Gaspard and D. Alonso, T. Okuda, and K. Nakamura, Phys. Rev. E **50**, 2591(1994).
- [18] P. Gaspard, “*Chaos, scattering and statistical mechanics*”, Cambridge University(1998).
- [19] P. Cvitanović, R. Artuso, R. Mainieri and G. Vattay, “*Classical and quantum chaos: a cyclist treatise*”(unpublished, 1998).
- [20] P. Cvitanović and B. Eckhardt, Phys. Rev. Lett. **63**, 823(1989); Nonlinearity **6**, 277(1993).
- [21] A. Wirzba, CHAOS **2**, 77-83(1992).
- [22] Y.-C. Lai, R. Blümel, E. Ott and C. Grebogi, Phys. Rev. Lett. **68**, 3491(1992).
- [23] B. Eckhardt, CHAOS **3**(4), 613(1993).
- [24] R. Blümel and U. Smilansky, Phys. Rev. Lett. **60**, 477(1988); Physica (Amsterdam) **D 36**, 111(1989); U. Smilansky, in *Chaos and Quantum Physics*, edited by M.-J. Giannoni, A. Voros, and J. Zinn-Justin (Elsevier

Science, New York, 1990), and references therein.

- [25] C. H. Lewenkopf and H. A. Weidenmüller, *Ann. Phys.* **212**, 53(1991).
- [26] T. Ericsson, *Phys. Rev. Lett.* **5**, 430(1960).
- [27] D. M. Brink and R. O. Stephen, *Phys. Lett.* **5**, 77(1963).
- [28] B. Eckhardt, G. Russberg, P. Cvitanović, P. E. Rosenqvist and P. Scherer, in “*Quantum chaos: between order and disorder*”, edited by G. Casati and B. Chirikov (Cambridge University Press, 1995).